A COMPARATIVE MODEL OF ECHOLOCATION JAMMING AVOIDANCE STRATEGIES IN BATS

John G Whitehead, Subhradeep Roy
Department of Engineering Science and Mechanics,
Virginia Polytechnic Institute and State University,
Blacksburg, VA, 24060
Email: {whijo23, sdroy } @vt.edu

ABSTRACT

Echolocation is a powerful active sensory system, but it is susceptibility to jamming. Jamming occurs when calls of similar frequency, time, and amplitude coincide resulting in misperceptions of the surroundings. One strategy for avoiding jamming found in bats is to lower the emission rate of echolocation calls and follow a neighbor. However, bats are known to move in large groups that do not have any consistent formation. It has been suggested that a higher emission rate strategy would be used in these large groups. This study aims to use numerical simulations of a two-dimensional agent-based model to compare the lower and higher emission rate strategies for efficacy of avoiding jamming to see if there is a need for changing strategies. A multi-vehicular model with collision avoidance that reaches an equilibrium state was generated to make this comparison. Jamming strategies were simulated by varying probabilities of using or not using a larger sensory area to avoid collisions. The model was run for groups of various sizes. The efficacy of each simulation was measured as the time of convergence at the equilibrium state, which is mandated to be a 2D circular trajectory. The results of the mean convergence times were compared within each group for variance with changes of probability and the mean convergence time at each probability and standard deviations were plotted to see if the variance was directional. Significant variance was found at groups of $4, 8, 16$, *and* 32 *agents, however none of these groups have significant directional trends. The model captures the salient features of the bat swarm motion, but within each simulation only a limited amount of jamming occurs, resulting in low influence of the avoidance strategies on the convergence time. The model will need to be readdressed in future work to increase the occurrence of jamming through increasing density instead of number of agents to better understand the relationship between the avoidance strategies and group size.*

1 INTRODUCTION

Echolocation is the use of ultrasonic waves to detect one's surroundings [1–4]. The waves are emitted at specific frequencies and the time and amplitude at which the waves return to the sender can provide the sender with information on the distance and size of objects around it. When these waves are emitted constantly at regular intervals, it allows the sender greater information as it can now track changes in its environment and detect movement, distance, and size [1]. There are a number of organisms that have made use of this active sensory system, but bats are particularly effective users of echolocation and use it to navigate and hunt in the dark [1–4]. However, echolocation has its limits. One limitation occurs when multiple bats of the same species (conspecifics) are using echolocation in the same area [2–5]. In this situation, the sound waves of each individual's calls become difficult to distinguish, making it hard for the bat to tell which returning echo is theirs. This can lead to misinterpretation of their environment based on their neighbors' calls. This misconception of their environment based on interpreting the wrong echo is called jamming.

To avoid jamming, bats employ a few different strategies. One is to change the frequency of their calls [3, 4]. By changing the frequency of their calls, they can avoid some of the distortion from calls of similar frequencies. Bats tend to show a preference to shift frequency calls up in the presence of conspecifics, but they can also shift their frequency down. Another documented strategies for jamming avoidance is to manipulate the emission rate of an individual's echolocation calls [2,5]. It has been shown that, in the presence of a few conspecifics, there is an average

decrease in the emission rate of the group. A study by Chiu et al. looked specifically at jamming avoidance in flying pairs and found that one member is greatly reducing their emission rate while the other calls regularly, resulting in the decrease in emission rate of the group [2]. This study also found that the member that lowers its emission rate closely follows the other bat. This would suggest that the bat with a lower emission rate is using fewer emissions to avoid jamming the other while following its partner to avoid collisions with its environment. This strategy works in small groups and could also work in larger ones if bats form smaller functioning groups of leaders and followers. Yet, when we look at the flight behavior of large groups, they fly in a non-uniform structure [6]. Therefore, we hypothesize that bats may use a completely different jamming avoidance strategy for the large group flight behaviors [7, 8].

Jarvis et al. recently demonstrated what this alternative may be [5]. They tested non-flying bats in the presence of simulated conspecific bat calls. When in the presence of several conspecifics, they found the same decrease in emission frequency previously documented. However, when they simulated calls from a large group, they found that the emission rate increased. This suggests that bats may have two different strategies to avoid jamming that they employ based on the number of conspecifics near them. In this work, we aim to use a two-dimensional agent-based model [9] and generate collective circular motion to compare the lower and higher emission rate strategies for efficacy of jamming avoidance strategies as observed in bats to understand each strategy's effectiveness at avoiding jamming in the presence of various numbers of conspecifics.

The paper is organized as follows. In Section 2, we describe the basic setup of the model to be used to replicate the bats' circular motion with a two-dimensional agent-based model and jamming avoidance through the use and disuse of a sensory region when jamming occurs. In Section 3, we provide the simulation results using the model in varying groups of agents and at a range of probabilities of disuse of the sensory region. In Section 4, we discuss the main results and its significance. In Section 5, we reiterate the results and discuss future work.

2 MODELING

This two-dimensional agent-based model creates a simplified version of a spiral flight behavior as demonstrated by some species of bats and uses the time it takes for the simulated bats to reach an equilibrium in this formation as a measure of efficacy for avoiding jamming [7].

The model is based on a multi-vehicular system, where the vehicles move at a constant velocity, starting from random initial positions, and move toward the goal of reaching a circular equilibrium motion around a beacon [9]. To look specifically at jamming avoidance, this model has been structured in two dimensions to put a limit on jamming avoidance through physical movement and spacing. Each bat is represented as a moving particle and has a keyhole shaped sensing area as shown in Figure 3, which represents the higher sensitivity region of echolocation in direction of a bat's velocity and an awareness of one's immediate surroundings [9, 10].

Jamming avoidance behaviors are modeled through a turning on and off of the pie shaped section of the keyhole, representing the echolocation beam. In the event of one vehicle detecting another in its echolocation beam, there is a probability p that the vehicle will not use its echolocation beam in the following time step. This allows for simulation of a decrease in emission rate to avoid jamming [2, 5]. Simulations are done with probabilities 0, 0.4, 0.76, and 1. Probability $p = 0$ represents a high emission rate jamming avoidance strategy (HER) as echolocation beams are used regardless of whether a chance for jamming is detected or not [5]. The other three are varying degrees of lower emission rate jamming avoidance strategies (LER). These values represent the probability of whether or not a bat will use its echolocation or be silent. Therefore, probability, $p = 1$ will always be silent, $p = 0.76$ is the highest frequency of occurrence of silent behavior documented, and $p = 0.4$ is the average occurrence [2]. Each probability is then simulated under different population sizes (n) on a logarithmic scale from 2^1 to 2^5 to assess the efficiency of these two strategies in different environments. The time for the system to converge to the equilibrium state around the beacon was used as an approximation of the effectiveness of the different strategies.

2.1 MODEL DESCRIPTION

To model multi-vehicular motion, we start with single vehicle case of which a schematic is in Figure 1. This involves the use of standard motion control laws as in [9], which are as follows:

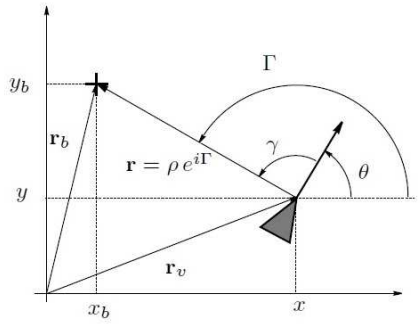

Figure 1: Schematic of single vehicle model at an instant, where the triangle is the vehicle and the cross denotes the fixed beacon [9].

$$\dot{x}(t) = v\cos\theta(t) \tag{1a}$$
$$\dot{y}(t) = v\sin\theta(t) \tag{1b}$$
$$\dot{\theta}(t) = u(t), \tag{1c}$$

where v is the velocity magnitude and is assumed to be constant and $t \in \mathbb{R}^+$ and is assumed to be discrete with an increment of $\Delta t \in \mathbb{R}^+$ in simulation. The vehicle state $[x, y, \theta]' \in \mathbb{R}^2 \times [-\pi, \pi)$ represents position of the vehicle at any time instant and $u(t)$ is the angular velocity, which acts as control input of the vehicle with respect to a fixed beacon [9], and is defined as follows

$$u(t) = \begin{cases} k\, g(\rho(t))\, \alpha_d(\gamma(t)), & \text{if } \rho(t) > 0 \\ 0, & \text{if } \rho(t) = 0 \end{cases} \tag{2}$$

where

$$g(\rho) = \ln\left(\frac{(c-1)\rho + \rho_0}{c\rho_0}\right) \tag{3}$$

and

$$\alpha_d(\gamma) = \begin{cases} \gamma, & \text{if } 0 \geq \gamma \leq \psi \\ \gamma - 2\pi, & \text{if } \psi < \gamma < 2\pi \end{cases} \tag{4}$$

In (3) and (4), ρ is the position of the vehicle from the beacon. Here, c, k and ρ_0 are constants and provided as input parameters. The parameter c influences the motivation or how fast the vehicle wants to reach at this equilibrium distance, and ρ_0 influences steady state distance from the equilibrium (ρ_e) [9]. The parameter α_d controls and influences the bat to move clockwise if it is too close to the beacon or counter-clockwise when it is too far away based on γ, the angle made by the heading of the vehicle and the direction of the beacon. The threshold of ψ, which must be equal to or greater than $(3\pi)/2$ is to ensure a constant rotational direction [9], counter-clockwise in the current model. We set ψ to be equal to $(11\pi)/6$. The parameter k influences the motivation of the vehicle, but in this case it is not a measure of its incentive to be at the equilibrium distance, but a measure of its willingness to change direction [9]. Both of these equations, (3) and (4), can be multiplied to generate the angular velocity, which in turn defines the control laws for the position of the bat [9].

In expanding this single model to a multi-vehicular model, as shown in Figure 2, the same equations are used to control the equilibrium distance and rotational movement. Terms are introduced to control the relationship of neighboring vehicles in addition to the pre-existing terms with respect to the beacon for single vehicle model. In other words, one addition is needed to

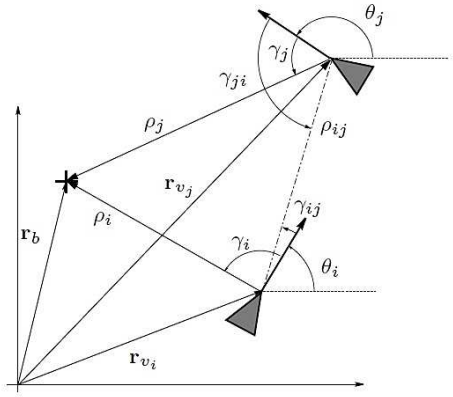

Figure 2: Schematic of multi vehicle model at an instant [9].

the single vehicle motion equations for an adjustment to u so that it is now a sum of the interactions between the vehicles and the beacon [9].

Consider a group of n agents whose motion is described by the kinematic equations

$$\dot{x}_i(t) = v\cos\theta_i(t) \tag{5a}$$
$$\dot{y}_i(t) = v\sin\theta_i(t) \tag{5b}$$
$$\dot{\theta}_i(t) = u_i(t), \tag{5c}$$

where $i = 1 \cdots n$. The control input $u_i(t)$ is modified with an additional term to incorporate the interaction between the $i-$th vehicle and any other perceived vehicle j as follows

$$u_i(t) = f_{ib}(\rho_i, \gamma_i) + \sum_{j \neq i,\ j \in \mathcal{N}_i(t)} f_{ij}(\rho_{ij}, \gamma_{ij}) \tag{6}$$

In (6), f_{ib} is same as that given in (2) for the single vehicle, where c is now replaced with c_b to specify the constant with respect to beacon and is given as follows

$$f_{ib}(\rho_i, \gamma_i) = \begin{cases} k_b.g(\rho_i, c_b, \rho_0).\alpha_d(\gamma_i), & \text{if } \rho_i > 0 \\ 0, & \text{if } \rho_i = 0 \end{cases} \tag{7}$$

The additional term f_{ij} is given by

$$f_{ij}(\rho_{ij}, \gamma_{ij}) = k_v.g(\rho_{ij}, c_v, d_0).\beta_d(\gamma_{ij}), \tag{8}$$

where, the input parameters $k_v > 0$, $c_v > 1$, $d_0 > 0$ and

$$\beta_d(\gamma_{ij}) = \begin{cases} \gamma_{ij}, & \text{if } 0 \geq \gamma_{ij} \leq \pi \\ \gamma_{ij} - 2\pi, & \text{if } \pi < \gamma_{ij} < 2\pi \end{cases} \tag{9}$$

Equation (8) is modeled similarly to that of (7), because it carries out a similar function of setting an optimal equilibrium point and a turning algorithm for controlling a vehicle, which is not at that equilibrium point. In this equation, g controls the distance not to the beacon, but to other vehicles and the equilibrium distance is d_0 [9].

The set $\mathcal{N}_i(t)$ is the set containing the index of the neighboring vehicles at time t residing inside the visibility region, which is the defined as the region the i-th vehicle can perceive other vehicles. It is noteworthy to mention that $\mathcal{N}_i(t)$ is time dependent.

2.2 SENSING SPACE AND COLLISION AVOIDANCE

With the addition of multiple vehicles, now collision avoidance is included [9]. The control laws for the multi-vehicle system is such that each agent i is driven by the term $f_{ib}(.)$ towards the counterclockwise circular motion about the fixed beacon and $f_{ij}(.)$ with two main aims: i) to achieve collision free trajectories between the vehicles and ii) to enforce the distance between any two vehicles, ρ_{ij}, to be equal to d_0. If $\rho_{ij} > d_0$, the $i-$th vehicle is attracted by any neighboring vehicle and if $\rho_{ij} < d_0$, the $i-$th vehicle is repulsed. Moreover, if $\rho_{ij} < d_s$, then the $j-$th agent is pushed outside the circular safety region around the $i-$th vehicle and thus avoiding collisions among the vehicles.

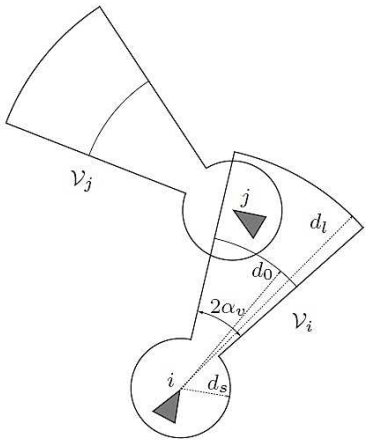

Figure 3: Sensing space for the vehicles [9].

Note that (8) is heavily dependent upon the sensing area. The keyhole formation is shown in Figure 3. In this sensory area, d_l is the full extent of the sensory region and jamming responses do not occur until the distance between reaches below d_l [9]. For this simulation d_l is always twice that of d_0 to represent the full extent a bat's echolocation beam of 10 m compared to the area of higher resolution used for small target detection of 5m [10].

2.3 JAMMING BEHAVIOR

The sensing area is split into two different sections relevant to jamming. First is a circle centered at the vehicle of radius d_s and it is always used to avoid collisions. Second, is the echolocation beam, which is represented by a sector of radius d_l $(d_l > d_s)$ with an angle of $2\alpha_v$. To simulate a low emission rate or silent behavior, probability values control the likelihood of the echolocation beam to not be used in the time step following jamming. Two probability values, $p = 0.4$ and $p = 0.76$, are chosen based on biological evidence for the average occurrence and highest occurrence of silence behavior in paired flight behavioral experiments [2]. The other, $p = 1$, is the extreme of every time jamming may occur the sensing space will be turned off for the next time step. Probability $p = 0$ signifies a high emission rate strategy as, no matter what happens with respect to jamming, the sensing area will always be used.

If another vehicle was detected within the area of d_0, there is a probability that in the following time step the bat will not use a sensing area and continue along its previous position trajectory of trying to reach ρ_e. If it does not perform a silence behavior, the bat will instead perform the previously programmed collision avoidance response of moving away from that neighbor. In this way, the model simulates a bat deciding to either continue a standard or relatively high emission rate and participate in physical avoidance responses or participate in a temporary low emission rate and follow a near neighbor to compensate for its own lack of sensory information [2]. If a bat continually participates in silence behavior and draws very near to a neighbor, collision will still be avoided due to the constant presence of the circular sensory region of d_s, regardless of jamming behavior.

3 SIMULATION RESULTS

For every simulation, starting from random initial position, there is a point at which the system reaches equilibrium state. This state is when all the vehicles are in a constant circular motion around the fixed beacon at the constant equilibrium distance ρ_e. This point is used as a measure of the efficacy of the jamming strategy in a particular group size, n. This rule functions within a low tolerance of 0.0001 to ensure we are finding the steady-state equilibrium point instead of a transient behavior.

First, we generate a circular motion model of a single vehicle. Figure 4 shows the resulting model and how one vehicle starts at the random position and then reaches to an equilibrium and remains executing circular motion about the fixed beacon which is origin in our model.

Next, this model was expanded to a multi-vehicular system and the vehicles are given random starting positions. Figure 5 shows two snapshots of the simulation of an 8 vehicle scenario. The first shows the vehicles moving towards the beacon from random positions at $t = 0$. The second shows the vehicles having reached the equilibrium state. In Figure 6, the mean angular distance $\bar{\gamma}$ and mean distance from the beacon, $\bar{\rho}$, are plotted to show when the equilibrium or convergence occurs in the simula-

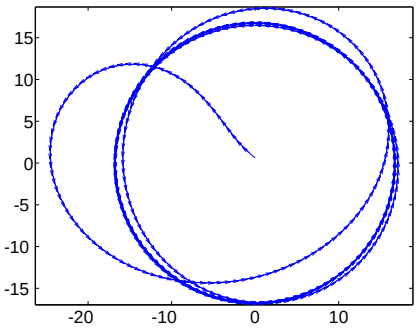

Figure 4: Trajectory of a single vehicle reaching to equilibrium

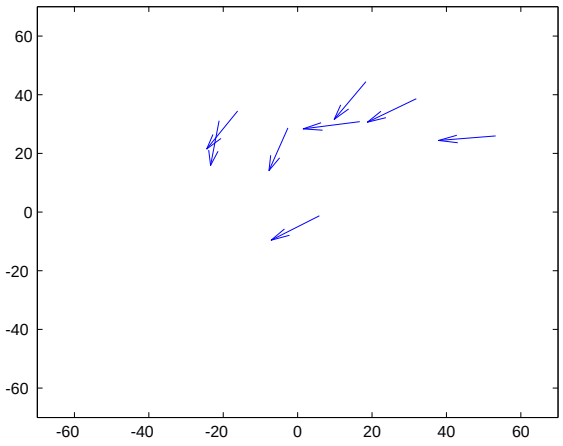

(a)

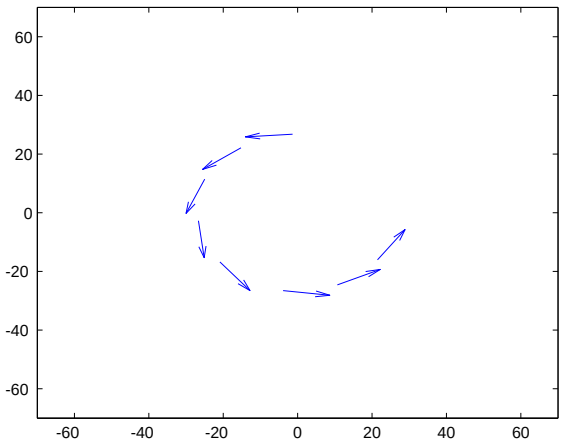

(b)

Figure 5: Eight vehicles reaching to equilibrium from random starting position. (a) $t = 0$. (b) $t = 2000$

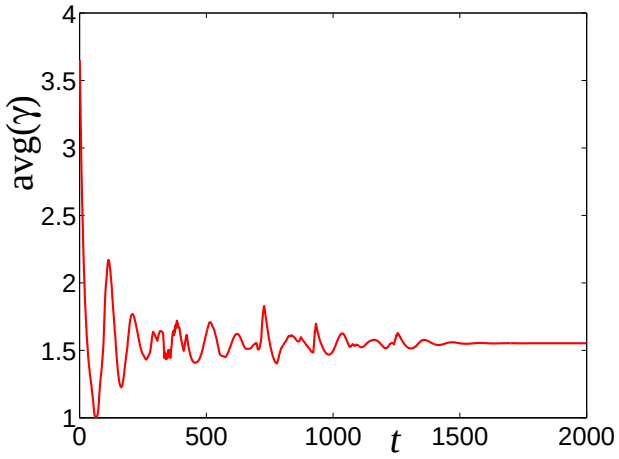

(a)

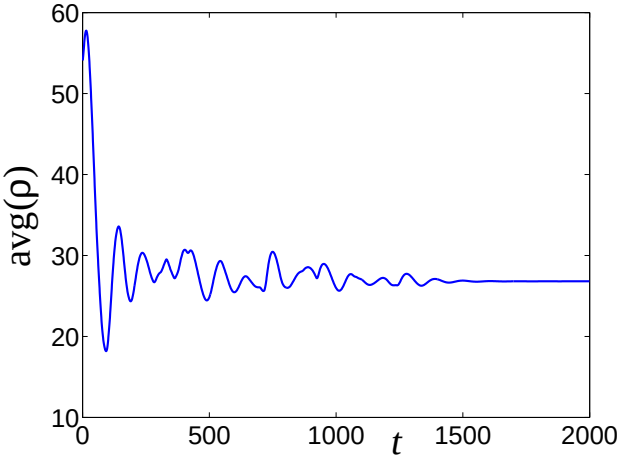

(b)

Figure 6: (a) Average angular distance reaches to equilibrium (b) Average distance from the beacon reaches to equilibrium

tion. At the equilibrium, the average of γ, the mean of the heading angles of the vehicles with respect to the beacon, reaches $\pi/2$, showing that the vehicles are moving perpendicular to the beacon. When the average of ρ is equal to ρ_e, the equilibrium state is reached. The analytical solution of ρ_e is provided in [9] as

$$\frac{v}{\rho_e} - k_b\, g(\rho_e)\, \frac{\pi}{2} = 0.$$

To ensure that jamming is occurring within the model the initial positions of the vehicles are fixed, n is held at 4, and the model is run for 100 simulations at various p's from 0.1 to 1. By limiting the only changing variable to p the probabilistic aspect of not using the echolocation beam after jamming will increase the variability in the time of convergence as p decreases. This

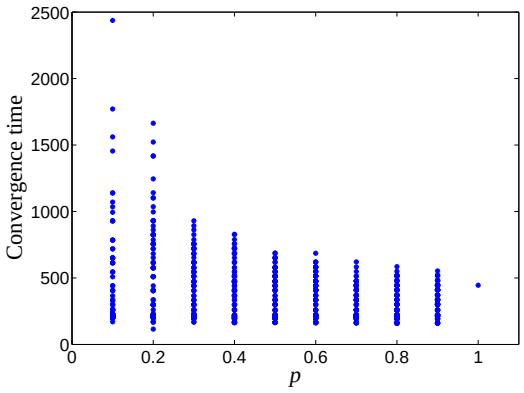

Figure 7: Convergence time for $n = 4$ with the change in probability values with fixed initial condition

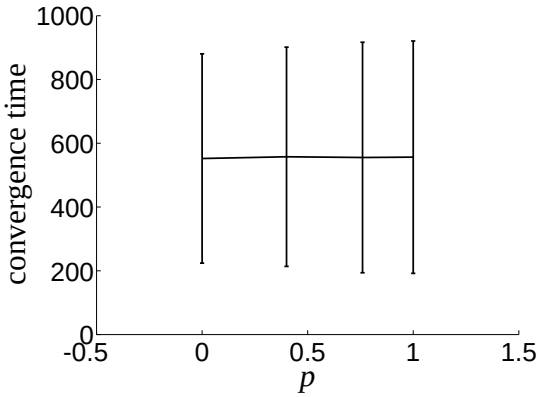

Figure 8: Mean and standard deviation of the convergence time for $n = 2$ with $10,000$ runs for $p = 0.1,\ 0.4,\ 0.76,\ 1$

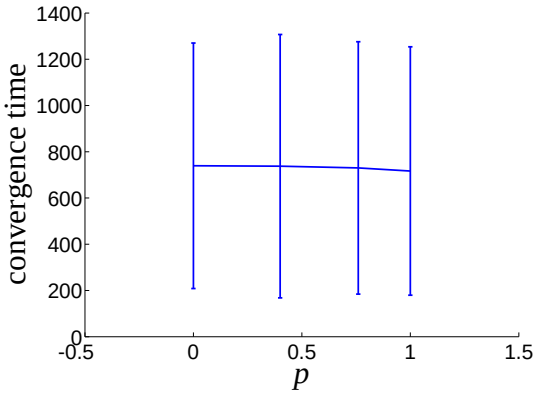

Figure 9: Mean and standard deviation of the convergence time for $n = 4$ with $10,000$ runs for $p = 0.1,\ 0.4,\ 0.76,\ 1$

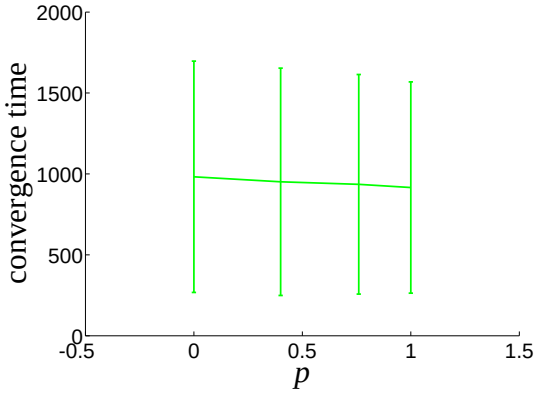

Figure 10: Mean and standard deviation of the convergence time for $n = 8$ with $10,000$ runs for $p = 0.1,\ 0.4,\ 0.76,\ 1$

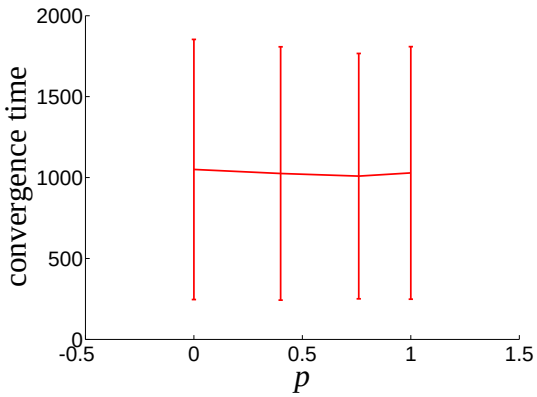

Figure 11: Mean and standard deviation of the convergence time for $n = 16$ with $10,000$ runs for $p = 0.1,\ 0.4,\ 0.76,\ 1$

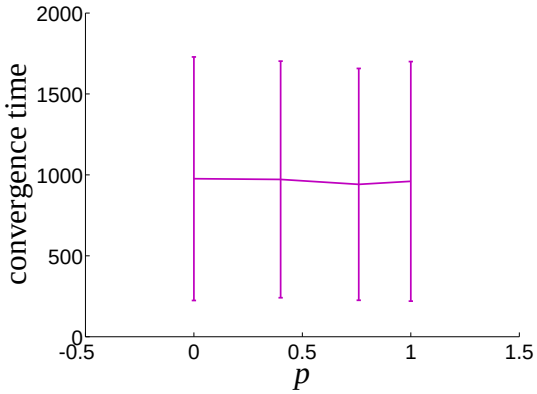

Figure 12: Mean and standard deviation of the convergence time for $n = 32$ with $10,000$ runs for $p = 0.1,\ 0.4,\ 0.76,\ 1$

leads to less consistency in the behavior of different runs of the simulation. Figure 7 plots the convergence times of those simulations at each p and clearly shows a strong increase in the variability of convergence time as the probability decreases from 1

(where no variation is apparent) to 0.1.

Finally, we ran 10,000 simulations of the model for each n (2, 4, 8, 16, 32) at each probability (0.0, 0.4, 0.76, 1.0). The results, in Figures 8, 9, 10, 11, and 12, show the mean time of convergence for each n at the different probabilities. One-way ANOVAs were used to see if the convergence time is dependent upon p within each n. As a result all of the ANOVAs have the same degrees of freedom between groups of 3 and within groups of 39,996. With an n of 2 the difference in convergence time did not vary based on the probability of jamming avoidance, ($F(3,39996) = 0.63$, 0.59). At $n = 4$, 8, 16, and 32, there was a significant effect of the probability of jamming avoidance on the convergence time, ($F(3,39996) = 4.19, < 0.01$; $F(3,39996) = 14.02, < 0.001$; $F(3,39996) = 3.69, = 0.01$; $F(3,39996) = 4.4, < 0.01$, respectively).

4 DISCUSSION

As shown in the results, we successfully generated a multi-vehicular model which started at random points and consistently reached the desired equilibrium state. We also managed to create a jamming effect within the system based on low emission rate behavior and it resulted in a change in the outcomes of the simulations. However, it is not clear that the different jamming avoidance strategies have any effect on the speed at which the model reaches equilibrium. The mean plots in Figures 8, 9, 10, 11, and 12 show very little change in time of convergence as the probability of silent behavior is increased at any n. Yet, statistically it is found that, at $n = 4$, 8, 16, and 32, there is significant variation in the mean convergence at different probabilities of silent behavior, < 0.05. At an $n = 2$ there is little to no significant difference in the mean convergence time when the jamming strategy changed, > 0.05. Even though statistically p has not influenced on the convergence time at $n = 4$, 8, 16, and 32, this does not mean that there is any specific trend. It only shows that changing the probability of silent behavior has a significant effect on the convergence time of the simulations.

These ambiguous results may be due to a lack of substantial jamming occurring within the model. We know that jamming is occurring, but we do not know how often. It may be that the lower emission rate jamming avoidance strategy does have an effect on the convergence time of the model, but due to the low frequency of occurrence of the behavior in comparison to normal movement the effect is diluted. This dilution would therefore increase as the amount of free space between the vehicles increases. You can see this in the p-values of the ANOVAs. An n of 2 may have an high p-value simply because the silent behavior hardly ever occurs within those simulations and therefore the probability has no effect on the convergence time. As n increases there is an increased significance in the p-values which reaches a minimum at an n of 8. This is most likely an artifact of the model. In the model ρ_e is not a constant, but varies based on d_0, ϕ, and n as

$$(n-1)\arcsin\left(\frac{d_0}{2\rho_e}\right)+\phi<\pi,$$

where

$$\phi=\min\{\alpha_v,\arcsin(\frac{d_l}{2\rho_e})\}.$$

Therefore, an n of 8 may be a situation where the ρ_e is relatively small compared to other n's creating a smaller circle for the equilibrium state, thereby increasing jamming within those simulations.

Interestingly, there are some suggestive trends as to the efficacy of the jamming avoidance strategies within the plots for n's of 4, 8, 16, and 32. All of which also had significant p-values for variance. The mean plots of both 4 and 8 have a slight downward trend from a p of 0, high emission rate, to a p of 1, extreme low emission rate. While the mean plots for 16 and 32 have a similar downward trend in convergence time from p of 0 to 0.76, but that reverses and the mean time increases at a p of 1. This would suggest that the low emission rate jamming avoidance strategy at frequencies found by Chui et al. [2] has greater efficacy than the high emission rate strategy through group sizes of 4 to 32. Yet, at the larger group sizes of 16 and 32, if silent behavior is practiced every time jamming is detected ($p = 1$) the low emission rate strategy does not have an advantage over the high emission rate strategy. This may be due to a decrease in the efficacy of the low emission rate strategy as the n increases. These aforementioned trends are not statistically significant, but they are intriguing and suggestive due to their consistency and because they exist with each n. Therefore, ρ_e remains the same as p is the only variable changing and it does not have an effect on ρ_e. This suggests these trends are not an artifact of the model itself, but may be trends generated by the changes in the probability of jamming avoidance behavior.

5 CONCLUSIONS

This model as it stands is inconclusive on the efficacy of the different jamming avoidance strategies. There is some suggestion that it is having some effect, due to the p-values and trends in some of the mean plots which show that the probability is having a strong effect on the variability between the groups and a possible downward trend in convergence time as the probability of silence behavior is increased. However, none of this is strong enough to be conclusive.

For future work, this model will have to be adjusted to decrease the space available between the vehicles and to measure how frequently jamming occurs. Then, it can be examined if the decrease in space, leads to an increase of jamming. A strong understanding of how to increase jamming within the model will allow for a re-examination of the efficacy of the different jamming

avoidance strategies in a system where jamming occurs with high frequency. This stronger presence of jamming in the simulations will allow for a clearer understanding of how changes in probability of silent behavior can influence convergence time of the system. Giving a better understanding of which jamming avoidance strategies are most effective for bats in different situations.

ACKNOWLEDGMENT

This work was supervised by Dr. Nicole Abaid and instructed by Dr. Shane Ross.

REFERENCES

[1] Arlettaz, R., Jones, G., and Racey, P. A., 2001. "Effect of acoustic clutter on prey detection by bats". *Nature,* **414**(6865), pp. 742–745.

[2] Chiu, C., Xian, W., and Moss, C. F., 2008. "Flying in silence: echolocating bats cease vocalizing to avoid sonar jamming". *Proceedings of the National Academy of Sciences,* **105**(35), pp. 13116–13121.

[3] Gillam, E. H., Ulanovsky, N., and McCracken, G. F., 2007. "Rapid jamming avoidance in biosonar". *Proceedings of the Royal Society B: Biological Sciences,* **274**(1610), pp. 651–660.

[4] Ulanovsky, N., Fenton, M. B., Tsoar, A., and Korine, C., 2004. "Dynamics of jamming avoidance in echolocating bats". *Proceedings of the Royal Society of London. Series B: Biological Sciences,* **271**(1547), pp. 1467–1475.

[5] Jarvis, J., Jackson, W., and Smotherman, M., 2013. "Groups of bats improve sonar efficiency through mutual suppression of pulse emissions". *Frontiers in physiology,* **4**.

[6] Theriault, D., Wu, Z., Hristov, N., Swartz, S., Breuer, K., Kunz, T., and Betke, M., 2010. Reconstruction and analysis of 3d trajectories of brazilian free-tailed bats in flight. Tech. rep.

[7] Herreid, C. F., and Davis, R. B., 1966. "Flight patterns of bats". *Journal of Mammalogy*, pp. 78–86.

[8] Williams, T. C., Ireland, L. C., and Williams, J. M., 1973. "High altitude flights of the free-tailed bat, *Tadarida brasiliensis*, observed with radar". *Journal of Mammalogy*, pp. 807–821.

[9] Ceccarelli, N., Di Marco, M., Garulli, A., and Giannitrapani, A., 2008. "Collective circular motion of multi-vehicle systems". *Automatica,* **44**(12), pp. 3025–3035.

[10] Bates, M. E., Simmons, J. A., and Zorikov, T. V., 2011. "Bats use echo harmonic structure to distinguish their targets from background clutter". *Science,* **333**(6042), pp. 627–630.